Articles

A New Class of Organic−Inorganic Sol−Gel Materials for Second-Order Nonlinear Optics

Ging-Ho Hsiue,*[,†,‡] Rong-Ho Lee,[†] and Ru-Jong Jeng[‡]

Department of Chemical Engineering, National Tsing Hua University, Hsinchu, Taiwan 300, ROC; Department of Chemical Engineering, National Chung Hsing University, Taichung, Taiwan 400, ROC

Received August 23, 1996. Revised Manuscript Received February 6, 1997[⊗]

A new class of organic/inorganic sol−gel second-order nonlinear optical (NLO) materials based on the prepolymer of hexakis(methoxymethyl)melamine (HMM) and an alkoxysilane dye (ASD) has been investigated. The NLO-active alkoxysilane dye containing nitroazobenzene was incorporated into the melamine matrixes with a weight ratio of 1:1. This organic−inorganic composite (HMM/ASD) was formed via sol−gel reaction of the respective components. The optically clear (HMM/ASD) sample exhibits large second-order optical nonlinearity (d_{33} = 40 pm/V) after poling and curing at 220 °C for 30 min. The poled/cured HMM/ASD sample has better temporal stability at 100 °C compared to that of the poled/cured ASD, due to its higher cross-linking density. This is confirmed by dielectric relaxation results indicating that the molecular mobility associated with the glass transition was suppressed remarkably for the cured HMM/ASD sample. Furthermore, the second harmonic generation (SHG) relaxations of these NLO-active sol−gel materials were studied via biexponential function curve-fitting.

Introduction

Second-order nonlinear optical (NLO) polymers have been widely studied for photonic applications such as frequency doubling and electrooptical (EO) modulation.[1,2] Large optical nonlinearity, low optical loss, and good temporal stability at elevated temperatures (60−125 °C) are required for these applications.[3] Different approaches have been investigated to prepare NLO-active polymers with excellent NLO properties.[3−12] One of these approaches is the sol−gel technique. Sol−gel materials for NLO applications are of interest for their low-temperature processing capability, excellent optical quality, good temporal stability, and ease of device fabrication.[8−12] For some NLO-active sol−gel materials, NLO-active dyes have been covalently incorporated into alkoxysilanes.[10−12] Subsequently, a three-dimensional inorganic network was prepared by the sol−gel processing of a NLO-active alkoxysilane dye. The inorganic network prepared by this process was designed not to compromise the stability of the organic components. Moreover, the network structure would restrict the randomization of poled (aligned) NLO chromophores and enhance the temporal stability of the second-order optical nonlinearity.

By incorporating the hardness of an inorganic sol−gel material into a high-performance organic polymer, the resulting hybrid organic/inorganic composite may display the desired properties of both components.[13−15] These composite types are capable of being fabricated into polymer films, which will not crack during the thermal process as typically observed in inorganic sol−gel systems.[16] Moreover, the incorporation of an inorganic sol−gel material provides an inert environment for the

* To whom all correspondence should be addressed.
† National Tsing Hua University.
‡ National Chung Hsing University.
⊗ Abstract published in *Advance ACS Abstracts*, March 15, 1997.

(1) Ermer, S.; Valley, J. F.; Lytel, R.; Lipscomb, G. F.; Vaneck, T. E.; Girton, D. G. *Appl. Phys. Lett.* **1992**, *61*, 2272.
(2) Prasad, P. N.; Williams, D. J. *Introduction to Nonlinear Optical Effects in Molecules and Polymers*; John Wiley & Sons, Inc.: New York, 1991.
(3) Xu, C.; Wu, B.; Todorova, O.; Dalton, L. R.; Shi, Y.; Ranon, P. M.; Steier, W. H. *Macromolecules* **1993**, *26*, 5303.
(4) Stenger-Smith, J. D.; Henry, R. A.; Hoover, J. M.; Lindsay, G. A.; Nadler, M. P.; Nissan, R. A. *J. Polym. Sci., Part A: Polym. Chem.* **1993**, *31*, 2899.
(5) Mandal, B. K.; Kumar, J.; Huang, J. C.; Tripathy, S. K. *Makromol. Chem., Rapid Commun.* **1991**, *12*, 63.
(6) Marturunkakul, S.; Chen, J. I.; Li, L.; Jeng, R. J.; Kumar, J.; Tripathy, S. K. *Chem. Mater.* **1993**, *5*, 592.
(7) Hsiue, G. H.; Kuo, J. K.; Jeng, R. J.; Chen, J. I.; Jiang, X. L.; Marturunkakul, S.; Kumar, J.; Tripathy, S. K. *Chem. Mater.* **1994**, *6*, 884.
(8) Kim, J.; Plawsky, J. L.; Laperuta, R.; Korenowski, G. M. *Chem. Mater.* **1992**, *4*, 249.
(9) Jeng, R. J.; Chan, Y. M.; Jain, A. K.; Kumar, J.; Tripathy, S. K. *Chem. Mater.* **1992**, *4*, 972.
(10) Yang, Z.; Xu, C.; Wu, B.; Dalton, L. R.; Kalluri, S.; Steier, W. H.; Shi, Y.; Bechtel, J. H. *Chem. Mater.* **1994**, *6*, 1899.
(11) Zhang, Y.; Prasad, P. N.; Burzynski, R. *Chem. Mater.* **1992**, *4*, 851.
(12) Wung, C. J.; Pang, Y.; Prasad, P. N.; Karasz, F. E. *Polymer* **1991**, *32*, 605.
(13) Landry, C. J. T.; Coltrain, B. K.; Brady, B. K. *Polymer* **1992**, *33*, 1486.
(14) Noell, J. L. W.; Wilkes, G. L.; Mohanty, D. K.; Mcgrath, J. E. *J. Appl. Polym. Sci.* **1990**, *40*, 1177.
(15) Landry, C. J. T.; Coltrain, B. K.; Wesson, J. A.; Zumbulyadis, N.; Lippert, J. L. *Polymer* **1992**, *33*, 1496.
(16) Yoshida, M.; Prasad, P. N. *Chem. Mater.* **1996**, *8*, 235.

S0897-4756(96)00445-0 CCC: $14.00

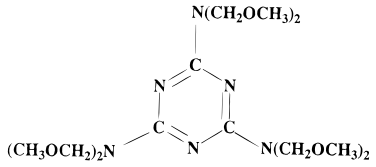

(a) HMM

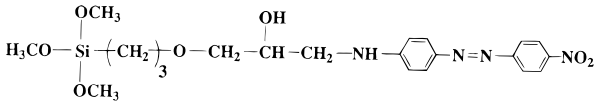

(b) ASD

Figure 1. Chemical structures of (a) HMM and (b) ASD, respectively.

organic polymer and theoretically will prevent its thermal decomposition. High optical transparency is obtained even after thermal cross-linking.[16] Landry et al. have reported that the interactions between an inorganic oxide and organic polymer reduced the molecular motions during the glass transition for the organic−inorganic sol−gel materials. Hydrogen bonding often occurs between the polymer chains and the residual hydroxyls on the surface of the SiO_2 network.[15] This is the predominant interaction for such organic−inorganic sol−gel materials. On the basis of the above consideration, the incorporation of an inorganic NLO-active sol−gel material with an organic polymer is a reasonable approach to enhance long-term NLO stability.

A melamine-based sol−gel material with its good transparency and a densely cross-linked network is a good candidate for the organic component of an NLO system.[6,17] Guest−host systems of melamine-based organic NLO-active sol−gel materials with low optical loss and high cross-link density have been developed in our laboratory.[18] In this study, a second-order NLO organic−inorganic sol−gel material based on the prepolymer of hexakis(methoxymethyl)melamine (HMM) and an alkoxysilane dye (ASD) has been prepared. The organic and inorganic networks were formed simultaneously during the sol−gel process. The temporal stability of this organic−inorganic sol−gel material (HMM/ASD) has been studied and compared with those of the cross-linked alkoxysilane dye (ASD) and the guest−host system of HMM/DO3 (DO3, Disperse Orange 3). Moreover, the SHG relaxation behaviors of these NLO-active materials have been studied by the biexponential function.[19,20] The phase homogeneity of these NLO-active sol−gel materials was analyzed by the temperature dependence on dielectric relaxation.

Experimental Section

Hexakis(methoxymethyl)melamine (HMM, Resimene 747, Figure 1a) was obtained from Monsanto and was used as received. A prepolymer of HMM (T_g = 2 °C) was prepared by heating the monomer at 220 °C for 1 h in the presence of an acid catalyst.[18] The alkoxysilane dye (ASD, Figure 1b) was synthesized by the coupling of a monoepoxy of (3-glycidoxypropyl)trimethoxysilane and a monoamine of 4-[(4′-nitrophenyl)azo]phenylamine (Disperse Orange 3).[21]

A prepolymer solution containing the ASD and HMM prepolymers was prepared for spin-coating. The ASD (0.1 g) and HMM prepolymers (0.1 g, weight ratio = 1:1) were dissolved in a mixed solvent (propylene glycol methyl ether acetate:1,4-dioxane = 3:1 by volume, 1 g), containing 20 mg of water and 20 mg of acetic acid to aid the hydrolysis of ASD and the HMM prepolymer. The prepolymer solution was stirred at room temperature for 4 h. Thin films were prepared by spin coating the polymer solution onto indium tin oxide (ITO) glass substrates.

The glass transition temperature (T_g) and the reaction behavior of the materials were determined by differential scanning calorimetry (DSC, Seiko SSC/5200) at a heating rate of 10 °C/min. The optimum curing conditions were determined by using the DSC isotrack technique. Degradation temperatures (T_d) were measured on a DuPont 951 thermogravimetric analyzer (TGA) at 10 °C/min under air. UV−vis spectra were recorded on a Hitachi 320 spectrophotometer. The cross-linking of the HMM/ASD sample was characterized by FTIR (Bio-Rad FTS155 FTIR). Scanning electron microscopy (SEM, Topcon ABT60) was used to study the morphology of the film (gold coated).

The dielectric relaxation behaviors of the NLO-active sol−gel materials were studied by dielectric spectroscopy (DEA, Novercontrol GmbH). The measurement was performed by using a Schlumberger SI 1260 impedance/gain-phase analyzer and a Quator temperature controller. For the dielectric measurement, the prepolymer solution was prepared in the same manner as for the spin-coating solution. The solution was cast onto the cell and dried at 60 °C for 3 h, followed by curing at 220 °C for 30 min. Dielectric measurements were made from 100 to 550 K. The frequency scan range was 10^{-1}−10^6 Hz.

The poling process for the second-order NLO polymer films was carried out using the in situ poling technique. The details of the corona poling setup were the same as was reported earlier.[22] The poling process was started at room temperature and increased to 220 °C at a heating rate of 15 °C/min. The corona current was maintained at 1 μA with a potential of 4.5 kV while the poling temperature was kept at 220 °C for 30 min. The formation of the network and the molecular alignment of the poled order proceeded simultaneously during this period. Upon saturation of the SHG signal intensity, the sample was then cooled to room temperature in the presence of the poling field, at which point the poling field was terminated. The typical thickness obtained was approximately 0.71 μm for the cured ASD/HMM sample. Indices of refraction at two different wavelengths (532 and 1064 nm) were measured using an ellipsometer. They were 1.70 and 1.63 at 532 and 1064 nm of the cured sample ASD/HMM, respectively. For the cured ASD, 1.60 (532 nm) and 1.54 (1064 nm) were obtained. Second harmonic generation measurements were carried out with a Q-switched Nd:YAG laser operating at 1064 nm. The relaxation behavior was studied by monitoring the decay of the effective second-order NLO coefficient, d_{eff}, as a function of time at 100 °C. Measurement of the second harmonic coefficient, d_{eff}, has been previously discussed,[23] and the d_{33} values were corrected for absorption.[24]

Results and Discussion

On heating the HMM/ASD sample at 220 °C for 30 min, the glass transition temperature (T_g) was vaguely observed near 110 °C from the DSC thermogram (Figure 2). The transition temperature of the cured HMM/ASD

(17) Brydson, J. A. Plastics Materials, 4th ed.; Butterworth Scientific: London, 1982.

(18) Jeng, R. J.; Hsiue, G. H.; Chen, J. I.; Marturunkakul, S.; Li, L.; Jiang, X. L.; Moody, R.; Masse, C.; Kumar, J.; Tripathy, S. K. *J. Appl. Polym. Sci.* **1995**, *55*, 209.

(19) Yu, W. C.; Sung, C. S. P. *Macromolecules* **1988**, *21*, 365.

(20) Firestone, M. A.; Ratner, M. A.; Marks, T. J.; Lin, W.; Wong, G. K. *Macromolecules* **1995**, *28*, 2260.

(21) Mandal, B.; Jeng, R. J.; Kumar, J.; Tripathy, S. K. *Makromol. Chem., Rapid Commun.* **1991**, *12*, 607.

(22) Hampsch, H. L.; Yang, J.; Wong, G. K.; Torkelson, J. M. *Macromolecules* **1990**, *23*, 3640.

(23) Jeng, R. J.; Chen, Y. M.; Kumar, J.; Tripathy, S. K. *J. Macromol. Sci., Pure Appl. Chem.* **1992**, *A29*, 1115.

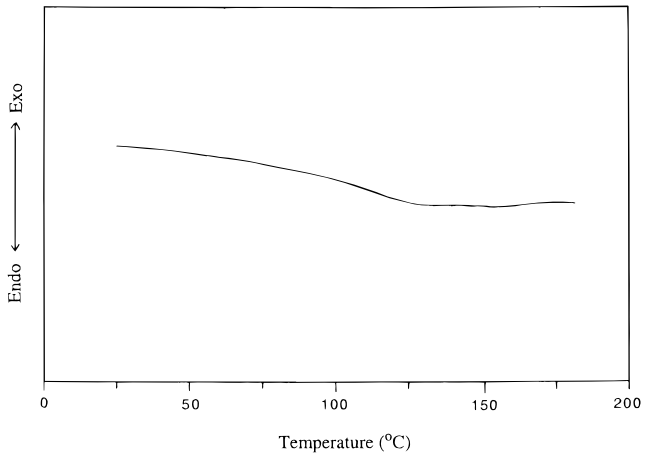

Figure 2. DSC thermogram of the cured HMM/ASD.

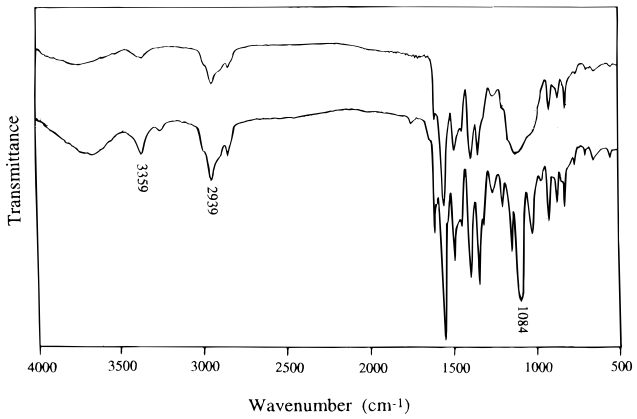

Figure 3. Infrared spectra of HMM/ASD, from bottom to top: pristine, cured.

was broad and the ΔCp (T_g) was small. This indicates the formation of a high cross-link density for the organic−inorganic network, resulting in a net decrease in both the chain mobility and vibrational contributions to Cp.[25−27] The curing temperature of 220 °C was chosen as the approximate midpoint between the start of exothermic curing (approximately 200 °C) and the thermal decomposition of ASD (approximately 237 °C).[28] Also, fabrication of second-order NLO polymer films requires simultaneous curing and poling. The thermal fluctuation at a high poling temperature would negatively affect the noncentrosymmetric alignment of the NLO chromophores. These additional factors were also taken into consideration in determining the optimum curing parameters. After curing of the HMM/ASD sample, the C−H vibrational stretch of the $O-CH_3$ and $O-CH_2$ groups at 2800−3000 cm^{-1} (for HMM) had decreased (Figure 3). This is due to condensation of the methoxymethyl groups.[29] In addition, the absorption peak at around 1100 cm^{-1} is much broader, suggesting Si−O−Si formation.[28] The above results are evidence for the formation of the organic (HMM) and inorganic

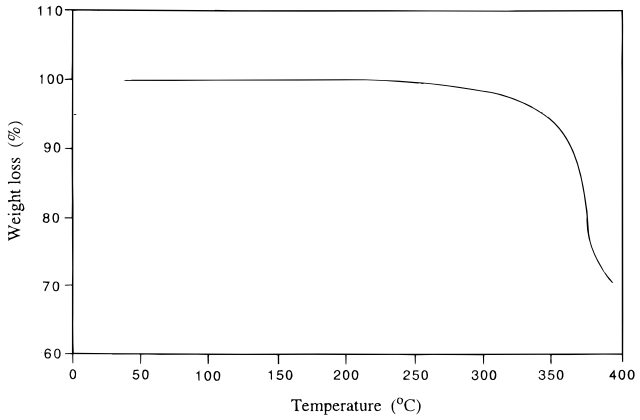

Figure 4. Thermal degradation behavior of the cured HMM/ASD.

(ASD) networks for cured HMM/ASD systems during the sol−gel process. In addition, the weak and broad peak corresponding to O−H stretching (in the Si−OH group) has been observed at 3500−4000 cm^{-1} for the cured HMM/ASD sample.[12] The residual hydroxyl groups on the surface of the SiO_2 network are the predominate source of interaction for these organic−inorganic sol−gel materials.[15] The cured HMM/ASD sample was soaked in the mixed solvent for 6 h, with no measurable extraction of the NLO-active dye as determined by UV/vis spectroscopy. This also confirms the formation of a highly cross-linked polymer network. A TGA scan of the cured HMM/ASD sample is shown in Figure 4. The cured HMM/ASD sample had an approximate T_d of 325 °C. The cured HMM/ASD sample has a higher T_d as compared to the cured ASD sample (291 °C), presumably due to a higher cross-linking density of the former.

Temporal stability of the second-order optical nonlinearity is related to the molecular mobility of the NLO chromophore. Broad-band dielectric spectroscopy is useful in studying the relaxation behavior of the NLO chromophore. The temperature dependence of the loss tan δ for the cured systems is given in Figure 5. For the cured HMM, the β-relaxation is attributed to the local (i.e., crankshaft) motion of the methylene or methylene-ether bridges in the network and the free motion of the dangling chains from the unreacted methoxymethyl groups.[30] The α-relaxation is observed near 65 °C (associated with the glass transition). The small amplitude of the α-relaxation implies a high cross-linking density of the cured HMM sample.[13] This results in the suppression of the large-scale and cooperative motions involved in the glass transition. For the cured HMM/DO3, the amplitudes of the β- and α-relaxations are slightly increased as compared to those of the cured HMM, due to a plasticizer effect. In Figure 5c, the spreading of the β-relaxation over a wide temperature range signifies the various motions of the chain segments for the cured ASD sample.[30] This relaxation is attributed to local and noncooperative motions of the NLO chromophores. The α-relaxation of the cured ASD was more significant compared to those of the cured HMM and HMM/DO3. This reflects the fact that the cured ASD sample has a lower cross-linking density. Moreover, the rigid NLO chromophore

(24) Mandal, B. K.; Chen, Y. M.; Lee, J. Y.; Kumar, J.; Tripathy, S. K. *Appl. Phys. Lett.* **1991**, *58*, 2459.
(25) Stevens, G.; Richardson, M. *Polymer* **1983**, *24*, 851.
(26) Plazek, D.; Frund, Z. *J. Polym. Sci., Part B: Polym. Phys.* **1990**, *28*, 431.
(27) Angell, C. A. *J. Non-Cryst. Solids* **1991**, *131*, 13.
(28) Jeng, R. J.; Chan, Y. M.; Jain, A. K.; Kumar, J.; Tripathy, S. K. *Chem. Mater.* **1992**, *4*, 1141.
(29) Daimay, L. V.; Norman, B. C.; William, G. F.; Jeanette, G. G. In *The Handbook of Infrared and Raman Characteristic Frequencies of Organic Molecules*; Academic Press, Inc.: San Diego, 1991; p 71.
(30) Betrabet, C. S.; Wilkes, G. L. *Chem. Mater.* **1995**, *7*, 535.

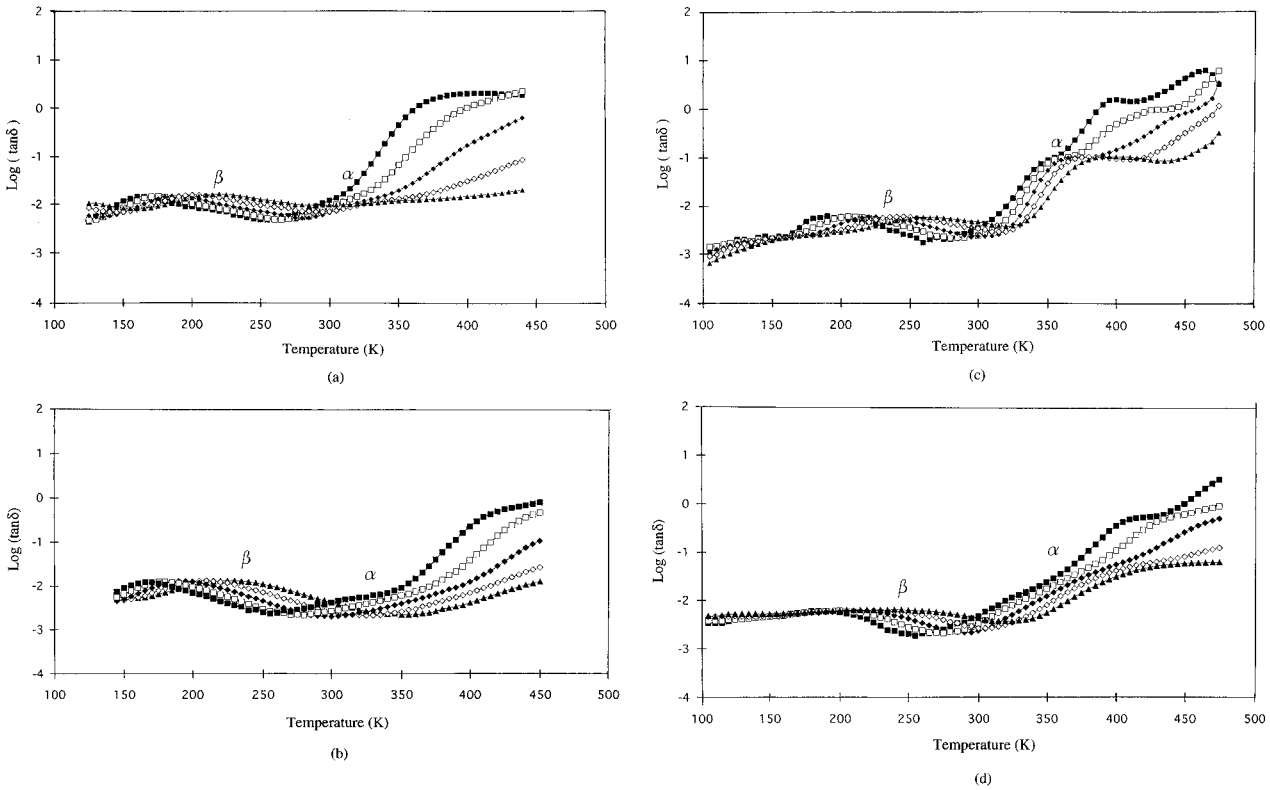

Figure 5. Temperature dependence of tan δ for cured (a) HMM, (b) HMM/DO3, (c) ASD, and (d) HMM/ASD, respectively. [10 (■), 100 (□), 1K (◆), 10K (◇), 100K (▲) Hz].

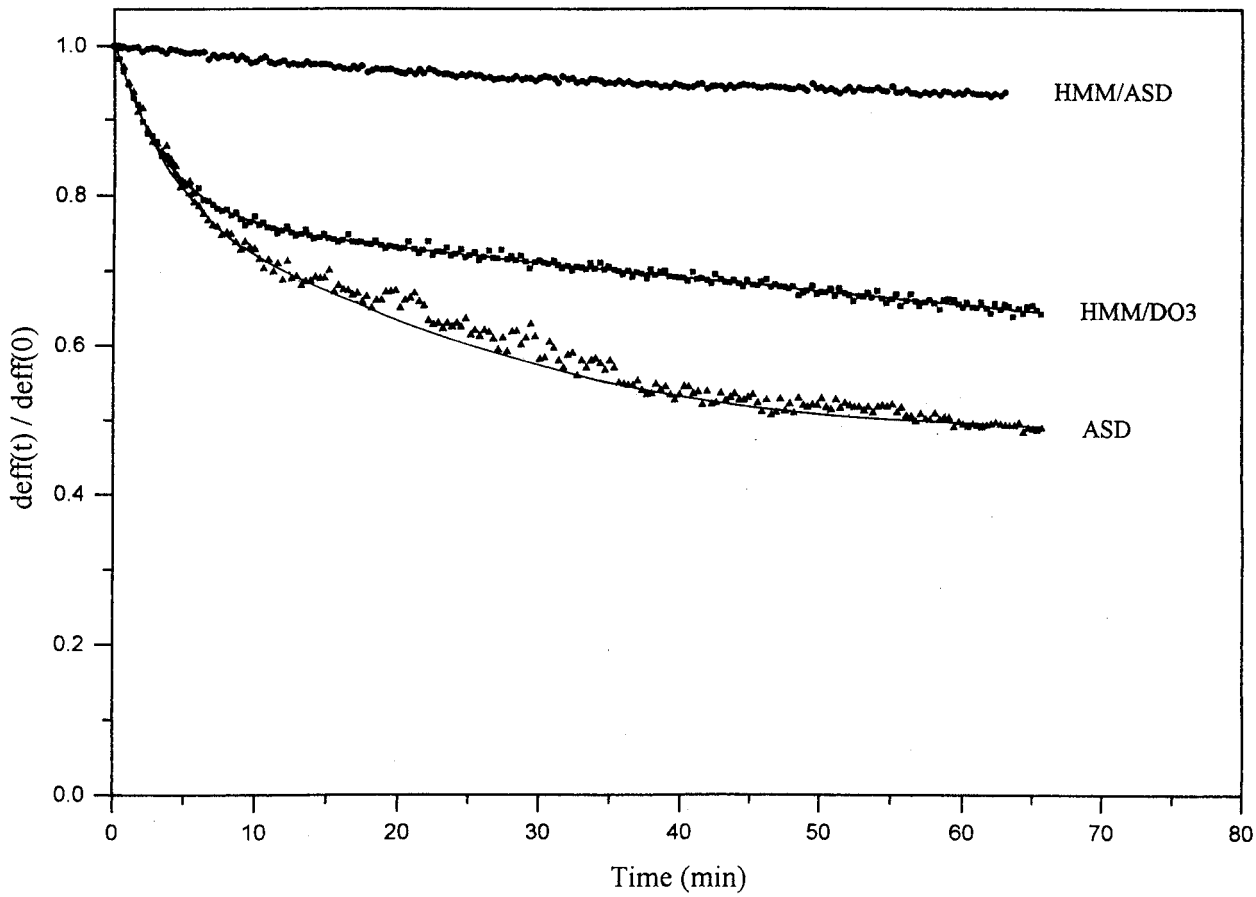

Figure 6. Temporal behavior of the effective second-order NLO coefficient of the poled/cured HMM/ASD (●), HMM/DO3 (■) and ASD (▲) at 100 °C (the solid line represents the curve fitting with eq 1).

was grafted to the network with the flexible methylene spacer, resulting in an increase of molecular mobility which involves the glass transition. The α-relaxation peak was broader for the cured HMM/ASD (Figure 5d) compared to that of the cured ASD sample. This broadening suggests that the organic chain segments

are densely and uniformly packed with the inorganic networks, leading to a reduction of the molecular motion in the cured ASD sample.[13,15] In addition, the β-relaxation and the relaxation which shows up above T_g are broader for the cured HMM/ASD sample (compared to those of the cured ASD sample). This reflects the fact that the mobility of the chain segments are also reduced because of the high cross-linking density for this organic−inorganic composite.

The temporal characteristics of the second harmonic coefficient (d_{33}) for the cured and poled HMM/ASD, HMM/DO3, and ASD films at 100 °C are shown in Figure 6. The poled/cured HMM/ASD and ASD samples exhibit d_{33} values of 40 and 54 pm/V, respectively. In Figure 6, a reduction of 7%, 35%, and 53% in d_{eff} value are observed for the poled/cured HMM/ASD, HMM/DO3, and ASD samples at 100 °C for 1 h, respectively. This indicates that the poled/cured HMM/ASD sample exhibits better temporal stability compared to that of the poled/cured ASD sample. This is due to the entrapment of NLO chromophores within the highly cross-linked organic−inorganic network. Moreover, optical clarity was maintained before and after the poling and curing process for this organic−inorganic composite. The homogeneity of this organic−inorganic composite is further confirmed using SEM. No sign of any phase separation was observed when the magnification was increased up to 40 K (Figure 7a). Moreover, the distribution of inorganic polymer networks (or chain segments) in the organic matrix has been further confirmed using SEM with a mapping technique (Figure 7b). The energy-dispersive X-ray microanalysis (EDAX) spectrum of the cured HMM/ASD sample suggests that the silicons is distributed uniformly through the polymer film and that the silicate particle sizes are much smaller than 1 μm.[31] This indicates that the inorganic networks are distributed uniformly throughout the polymer film on the molecular scale for the cured HMM/ASD sample. Optical microscopy reveals a clear, transparent, and featureless film as well.

In addition, the SHG relaxation behaviors of the poled/cured HMM/DO3 and ASD samples have been fit by a biexponential function (eq 1).[19,20] The relaxation process can be broken down into the faster and slower relaxation components:[19,20]

$$\phi(t) = C_f e^{-(t/\tau_f)} + C_s e^{-(t/\tau_s)} \quad (1)$$

Here the ϕ and τ represent the normalized decay of the effective second-order NLO coefficient and relaxation time, respectively. The C_f and C_s are coefficients describing the fractions of the fast and slow relaxation processes. Curve fitting for the SHG relaxations are summarized in Table 1. The equation fits the decay curves very well only for the poled/cured HMM/DO3 and ASD samples. For the poled/cured HMM/ASD sample, the SHG decay could not be fit with a biexponential function and attempted fits resulted in large deviations from the data. This is because significant decay of the SHG was not observed for poled/cured HMM/ASD, due to its high cross-linking density. The extremely slow decay of the SHG data corresponds to very long relaxation times. This phenomenon also has been reported by Chen et al.[32] The cured ASD sample exhibits a longer relaxation time than the cured HMM/DO3 for both the fast and slow relaxations. This is because the chromophore (DO3) of ASD is grafted directly onto the inorganic networks, leading to a reduction of motion of the chromophore. Therefore, longer relaxation times were observed for these two relaxation processes. Moreover, the sum of the C_f and C_s coefficients is nearly unity, which reflects the fact that the biexponential function is suitable for curve fitting of the SHG relaxations. The fraction of the fast relaxation (C_f) for the poled/cured ASD sample is larger than that for the HMM/DO3 sample. This implies that the poled/cured ASD has a larger cumulative area of free volume than

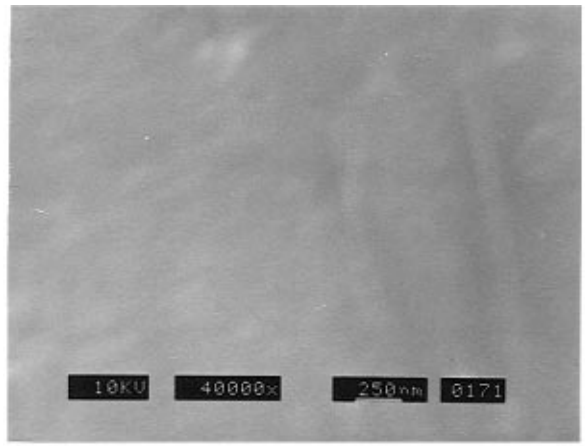

(a)

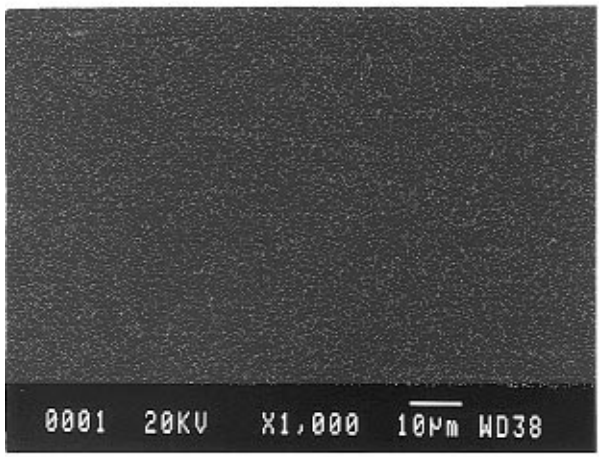

(b)

Figure 7. (a) Scanning electron micrograph and (b) energy-dispersive X-ray microanalysis (EDAX) spectrum of the cured HMM/ASD sample.

Table 1. Kinetic Data of SHG Decay Collected from the Curve Fitting with Biexponential Function for Poled/Cured HMM/DO3, ASD, and HMM/ASD

sample	C_f	τ_f (min)	C_s	τ_s (min)
HMM/DO3	0.23	3.5	0.77	367.6
ASD	0.36	16.0	0.58	380.5
HMM/ASD	nd[a]	nd	nd	nd

[a] Data could not be obtained.

(31) Premachandra, J.; Kumudinie, C.; Zhao, W.; Mark, J. E. *J. Sol−Gel Sci. Tech.* **1996**, *7*, 163.

(32) Chen, J. I.; Marturunkakul, S.; Li, L.; Jeng, R. J.; Kumar, J.; Tripathy, S. K. *Macromolecules* **1993**, *26*, 7379.

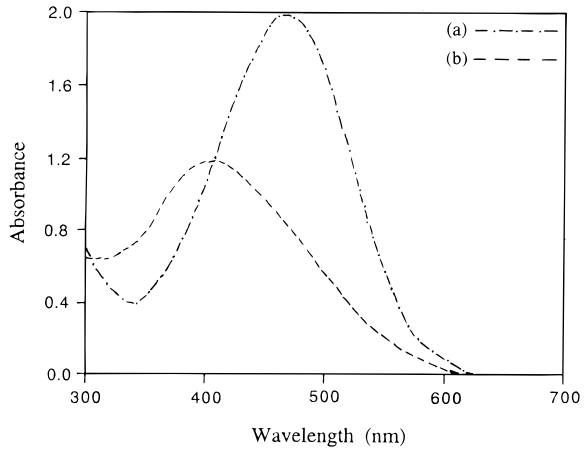

Figure 8. UV/vis absorption spectra of the HMM/ASD: (a) pristine; (b) immediately after poling/curing process.

the HMM/DO3, with the assumption that the critical size of the free volume is large enough for fast relaxation. This result agrees with the dielectric relaxation analysis showing that the cured ASD sample has a lower cross-linking density than the HMM/DO3 sample. Consequently, the temporal stability of the poled/cured ASD sample is poorer than that of the poled/cured HMM/DO3 sample. In addition, the influence of the poling effect on the absorption behavior of the HMM/ASD sample has been studied by UV/vis spectroscopy. The absorption spectra for a HMM/ASD sample before and after the poling/curing process are shown in Figure 8. Immediately after poling/curing, a decrease in absorbance was observed. This is likely due to dye degradation (or sublimation) and orientational dichroism.[10,18] The absorption peak of the ASD chromophore shifted toward a shorter wavelength. This behavior is similar to that observed in other cross-linked NLO polymer systems.[3,18,24]

Conclusion

A novel organic−inorganic sol−gel material for second-order nonlinear optics has been developed. This cross-linked HMM/ASD composite is optically clear with no sign of phase separation as determined by SEM. The EDAX spectrum shows uniformly distributed silicon within this organic−inorganic composite film. The poled/cured HMM/ASD sample exhibits a large second-order optical nonlinearity (40 pm/V). The molecular relaxation associated with the glass transition was remarkably suppressed for the cured HMM/ASD sample as determined by dielectric analysis. Moreover, the organic chain segments are densely and uniformly packed throughout the inorganic network as is suggested by the broadening of the α-relaxation peak. Better temporal stability at 100 °C is obtained for the poled/cured HMM/ASD sample compared to that of the cured ASD sample, due to a higher cross-linking density.

Acknowledgment. The authors thank the National Science Council of Taiwan, ROC for financial support (Grant NSC85-2216-E007-046). Thanks are also due to Dr. J. E. Kemnitzer of Integra Lifesciences Corp. for technical editing.

CM960445F